*6198–6209* *Nucleic Acids Research, 2020, Vol. 48, No. 11* *Published online 7 May 2020*
*doi: 10.1093/nar/gkaa313*

# Group II intron as cold sensor for self-preservation and bacterial conjugation

**Xiaolong Dong[1,†], Guosheng Qu[2,*,†], Carol Lyn Piazza[1] and Marlene Belfort[1,*]**

[1]Department of Biological Sciences and RNA Institute, University at Albany, Albany, NY 12222, USA and [2]College of Life Sciences, Hebei University, Baoding, Hebei 071002, China

Received December 15, 2019; Revised April 01, 2020; Editorial Decision April 16, 2020; Accepted April 20, 2020

## ABSTRACT

**Group II introns are self-splicing ribozymes and mobile genetic elements. Splicing is required for both expression of the interrupted host gene and intron retromobility. For the pRS01 plasmid-encoded *Lactococcus lactis* group II intron, LI.LtrB, splicing enables expression of the intron's host relaxase protein. Relaxase, in turn, initiates horizontal transfer of the conjugative pRS01 plasmid and stimulates retrotransposition of the intron. Little is known about how splicing of bacterial group II introns is influenced by environmental conditions. Here, we show that low temperatures can inhibit LI.LtrB intron splicing. Whereas autocatalysis is abolished in the cold, splicing is partially restored by the intron-encoded protein (IEP). Structure profiling reveals cold-induced disruptions of key tertiary interactions, suggesting that a kinetic trap prevents the intron RNA from assuming its native state. Interestingly, while reduced levels of transcription and splicing lead to a paucity of excised intron in the cold, levels of relaxase mRNA are maintained, partially due to diminished intron-mediated mRNA targeting, allowing intron spread by conjugal transfer. Taken together, this study demonstrates not only the intrinsic cold sensitivity of group II intron splicing and the role of the IEP for cold-stress adaptation, but also maintenance of horizontal plasmid and intron transfer under cold-shock.**

## INTRODUCTION

Group II introns are self-splicing ribozymes that are believed to be progenitors of eukaryotic spliceosomal introns and retroelements (1,2). The splicing process involves two consecutive transesterification steps giving rise to a free intron lariat and ligated exons (1) (Figure 1A). This reaction can be carried out by the RNA itself under high concentrations of salt and magnesium. In the cell or under physiological conditions *in vitro*, splicing requires a protein encoded by the intron itself. This intron-encoded protein (IEP) is translated from an open reading frame (ORF) that is looped out of the intron's catalytic core. IEP binding allows stabilization of tertiary interactions within the intron RNA under low salt and magnesium conditions (3,4). In addition to maturase activity that is required for the intron's folding and splicing, the IEP also possesses reverse transcriptase activity, which is responsible for copying the intron RNA into DNA during retromobility (1).

Although varying in primary sequence, group II introns are highly conserved in secondary and tertiary structure (5). The intron RNA is organized into six domains, DI-DVI (Figure 1B). DI is the largest and the first to be transcribed and folded. This domain contains numerous key motifs involved in an extensive network of tertiary interactions, including α–α′ and β–β′, which are essential for the entire RNA to fold. DI also harbors the exon-binding sequences (EBSs) that base-pair with intron-binding sequences (IBSs) within the intron's flanking exons. Folding of DI is modulated by a regulatory element in the κ–ζ region (Figure 1B), proper formation of which is early, magnesium-dependent, kinetically controlled and rate-limiting for tertiary collapse of the entire ribozyme (6–8). Well-folded DI provides a scaffold for the remainder of the intron to fold and connects through tertiary interactions with other domains (5). DII and DIII contribute structurally to the intron RNA by interacting respectively with DVI and DV, both of which are essential for catalysis. DIV contains the ORF that encodes the IEP, as well as a high-affinity anchoring site for this protein after its translation. The highly conserved DV is the catalytic domain that harbors the core of the active site. DVI is immediately upstream of the 3′-end of the intron RNA and contains the bulged adenosine, which initiates the nucleophilic attack that drives the first transesterification reaction. So far, various crystal structures of the intron RNA alone and a few cryo-electron microscopy (cryo-EM) structures of the intron as RNA-protein complexes have been reported, all demonstrating a well-packed intron RNA (9–14).

*To whom correspondence should be addressed. Email: mbelfort@albany.edu
Correspondence may also be addressed to Guosheng Qu. Email: guosheng.qu@yahoo.com
†The authors wish it to be known that, in their opinion, the first two authors should be regarded as Joint First Authors.

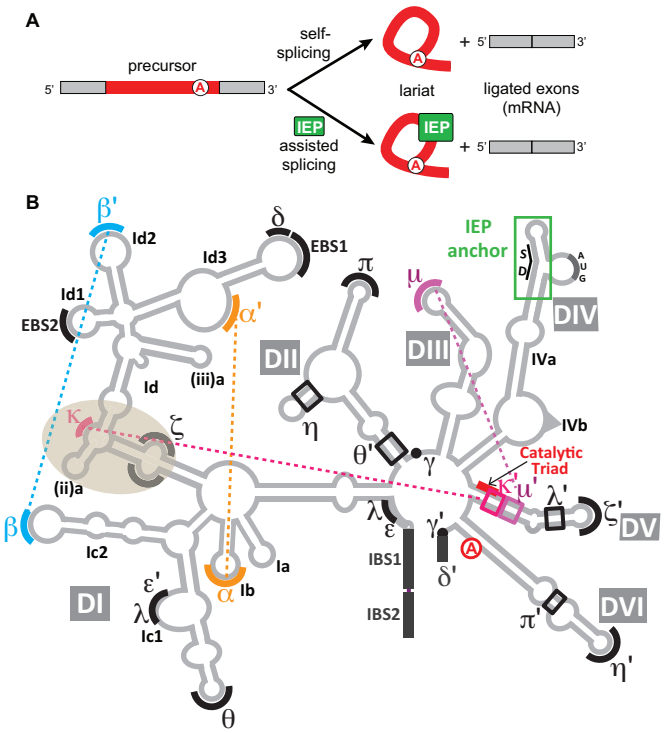


**Figure 1.** Group II intron splicing and structure. (**A**) The splicing pathway under self-splicing and IEP-assisted conditions. In both pathways, the intron (red) undergoes the same two consecutive transesterification steps, releasing the intron in the lariat form and ligating the two exons. Circled red 'A' denotes the branch point. Green blocks denote the IEP. (**B**) Secondary structure of the group II intron Ll.LtrB. The intron RNA is depicted in grey. Domains are labeled as DI-DVI along with their subdomains. Major tertiary interaction motifs are labeled in Greek characters, with key interactions highlighted by dotted lines (orange, cyan, hot pink and purple for α–α′, β–β′, κ–κ′ and μ–μ′, respectively). The κ–ζ region is indicated by the brown bubble. The catalytic triad in DV is indicated in red. IEP anchor site is indicated by the green box. EBS: exon-binding sequence, IBS: intron-binding sequence, SD: Shine-Dalgarno Sequence, AUG: translation start codon.

Group II introns occur in all domains of life (2). As mobile retroelements, most of them can spread themselves in the cell by invading DNA. Some group II introns can also disseminate horizontally through mobilization of other mobile elements with which they cohabit (15). Nevertheless, group II introns are only found in a limited number of bacteria, archaea and organelles of eukaryotes (2). In addition to the strong selective pressure against 'junk' DNA in bacterial genomes (16), a recent study showing that group II introns can inhibit host gene expression provides another possible explanation for the paucity of group II introns in contemporary organisms (17). Furthermore, the relative rarity of group II introns might also be explained by having been challenged by environmental conditions that drove them either to evolve or to be lost. It is therefore important to understand how group II introns respond to and survive environmental challenges.

In this study, we examined the *Lactococcus lactis* LtrB (Ll.LtrB) group II intron residing on a conjugative plasmid pRS01. The intron's host gene *ltrB* encodes a relaxase protein that is responsible for the plasmid's conjugal transmission (18). We found that splicing of the group II intron is sensitive to cold and that such sensitivity can be rescued by the IEP. Thus, this work supports the notion that cognate protein partners play fundamental roles in adaptation of ribozymes to unfavorable environmental conditions. We also demonstrate that relaxase mRNA levels are maintained at least partially because the reduction in excised intron minimizes degradative mRNA targeting. The result is that in the face of cold stress, which shuts down cellular processes, there is continued conjugal transfer of the plasmid with its resident intron, ensuring the persistence of both these mobile elements.

## MATERIALS AND METHODS

### Strains and growth conditions

Ll.LtrB was expressed in the native host *L. lactis* strain IL1403 either constitutively (from pDL278 plasmid) or after nisin induction (from pCY20 plasmid, Supplementary Table S1) as previously described (17). Cultures were grown in GM17 media (M17 broth supplemented with 0.5% glucose) in tightly-capped tubes or bottles at 30°C without aeration. Where suitable, the media contained spectinomycin (Spc) at 300 μg/ml, chloramphenicol (Cam) at 10 μg/ml, erythromycin (Erm) at 10 μg/ml, or fusidic acid (FA) at 25 μg/ml. The cell culture was initiated at 30°C. When the $OD_{600}$ reached 0.5–0.6, the culture was shifted to lower (10°C or 20°C) or higher temperatures (40°C) in water baths for 10 min and grown for an additional 3 h (with the pCY20 strains induced with 0.4 μg/ml nisin). Analysis of EcI5 and BhI1 group II intron expression in *Escherichia coli* was performed as described previously (17). Briefly, *E. coli* MC1061 cells containing pET11a (Supplementary Table S1) expression plasmids were grown to $OD_{600}$ 0.3, induced with 100 μM IPTG and grown in LB media with 100 μg/ml ampicillin at shifted temperatures with 250 rpm shaking for an additional 3 h.

### Stress growth conditions

Anaerobic growth: Cultures were grown under regular conditions except that every step was completed in an anaerobic chamber. Aerobic growth: Cultures were grown in loose-cap tubes at 30°C with continuous shaking at 250 rpm for 3 h. Log phase growth: Cultures were grown under regular conditions until $OD_{600}$ ~0.3 and then induced for 3 h. UV treatment: Cultures were grown under regular conditions until $OD_{600}$ ~0.3, exposed to UV irradiation (10 000 μJ/cm$^2$; 5 ml culture in a 60 × 15 mm petri dish), and then induced for 3 h. 10°C and 42°C: Cultures were grown to $OD_{600}$ 0.5–0.6 under the regular conditions and then incubated at defined temperatures for 3 h after nisin was added. Glucose deprivation: M17 media was used without glucose. Osmotic shock: regular media supplemented with 0.6 M NaCl. Heavy metal stress: regular media supplemented with 0.2 mM copper(II) sulfate. Cultures were grown to $OD_{600}$ 0.5–0.6 under regular conditions, spun down, and resuspended in corresponding media and induced at 30°C for 3 h.

### Ll.LtrB IEP purification

The protein purification method was as previously described using the expression plasmid pImp-1P (Supplementary Table S1) containing the IEP ORF along with a bridging intein and a chitin-binding domain (19). Briefly, *E. coli* BL21(DE3) cells containing the plasmid were grown in LB media containing 100 μg/ml ampicillin to $OD_{600}$ 0.6 at 37°C and induced with 100 mM IPTG at 25°C for an additional 6 h. The cells were collected and lysed. The cleared lysate was loaded onto a chitin column (New England Biolabs) and the protein product was obtained by dithiothreitol (DTT)-induced cleavage of the intein. The protein was then buffer exchanged with the RNP buffer (100 mM KCl, 5 mM $MgCl_2$, 20 mM Tris–HCl (pH 7.5) and 1 U/μl murine RNase-inhibitor (New England Biolabs)) containing 25% glycerol, concentrated using an Amicon Ultra 15 ml centrifugal filter and snap frozen for storage at −80°C.

### Intron splicing *in vitro*

The Ll.LtrB intron precursor RNA (the 902-nt ΔORF ribozyme flanked by short IBS-containing exons, which are 27 nt and 26 nt for the 5′ and 3′ exons, respectively) was synthesized by *in vitro* transcription with a Megascript T7 transcription kit (Ambion) using a DNA template described previously (20). The RNA was recovered by Monarch purification columns (New England Biolabs), dissolved in water and heated at 65°C for 5 min immediately before use.

For self-splicing, the RNA was denatured at 65°C for 5 min and preincubated at appropriate temperatures for 30 min along with the 2× self-splicing buffer (3 M $NH_4Cl$, 100 mM $MgCl_2$, 80 mM Tris–HCl (pH 7.5) and 10 mM DTT). The RNA (5 μg) was then mixed with the 2× buffer in a 1:1 (v:v) ratio for a final concentration of 1.5 M $NH_4Cl$, 50 mM $MgCl_2$, 40 mM Tris–HCl (pH 7.5) and 5 mM DTT and incubated for 3 h. The reaction was terminated by adding ice-cold 100% ethanol to precipitate the RNA for analysis by primer extension or on an 8% urea/polyacrylamide gel stained with SYBR Green (Thermo Fisher).

For IEP-assisted splicing, the RNA (5 μg) was denatured at 65°C for 5 min and preincubated at appropriate temperatures for 30 min. The IEP (10 μg) and the 2× RNP buffer (200 mM KCl, 10 mM $MgCl_2$, 40 mM Tris–HCl (pH 7.5) and 2 U/μl murine RNase-inhibitor) were also preincubated at same temperatures for 30 min. The RNA, the IEP and the 2× buffer were then mixed 1:2:1 (v:v:v) to reach a final concentration of 100 mM KCl, 5 mM $MgCl_2$, 20 mM Tris–HCl (pH 7.5) and 1 U/μl murine RNase-inhibitor and incubated for 3 h. The reaction was terminated by adding chilled phenol and immediate vortexing, followed by phenol/chloroform extraction and ethanol precipitation for further analysis.

### Reverse transcription primer extension

Total RNA was obtained from cell pellets by phenol/chloroform extraction. Primer extension was done using SuperScript III Reverse Transcriptase (Thermo Fisher), according to manufacturer's instructions, with 4 μg of RQ1 DNase (Promega)-treated RNA and 0.4 pmol of oligonucleotide primers (IDT1073, IDT6823 and IDT6828 for Ll.LtrB, BhI1 and EcI5 introns, respectively) (Supplementary Table S2). Primers were labeled with γ-$^{32}$P (PerkinElmer) using T4 Polynucleotide Kinase (New England Biolabs). For the primer extension termination assay, ddTTP was added to replace dTTP in the reaction for detection of intron precursor and spliced intron. Products were separated on a 6% urea/polyacrylamide sequencing gel, which was exposed on a phosphor screen and scanned on a Typhoon Trio (GE Healthcare). The quantitation was done using ImageQuant (GE Healthcare).

### Gel mobility shift assay

The intron RNA and the IEP were mixed as described above and incubated in the RNP buffer (100 mM KCl, 5 mM $MgCl_2$, 20 mM Tris–HCl (pH 7.5) and 1 U/μl murine RNase-inhibitor) at 10°C or 30°C for 3 h. The mixture was then analyzed on a 4% native polyacrylamide gel run at 4°C followed by SYPRO Ruby staining (Thermo Fisher) according to manufacturer's instructions.

### Selective 2′-hydroxyl acylation analyzed by primer extension (SHAPE)

For *in vitro* SHAPE in the presence of the IEP, 80 mM 1-methyl-6-nitroisatoic anhydride (1M6) dissolved in DMSO was added 1:9 (v:v) to the IEP-assisted splicing reaction for a final concentration of 8 mM at each temperature. The reactions were incubated for 10 min before cold phenol/chloroform was added for RNA extraction (4).

For *in vitro* SHAPE in the absence of the IEP, the same concentration of 1-methly-7-nitroisatoic anhydride (1M7) was used in addition to 1M6. The RNA was recovered by adding cold 100% ethanol at the end of the reactions and immediately put at −80°C for precipitation. After primer extension using intron-specific oligonucleotide primers (Supplementary Table S2), separation was achieved on a 6% urea/polyacrylamide sequencing gel. Quantitation was as described previously (4).

### Northern blot

Northern blots were prepared as previously described (17). Briefly, 7.5 μg of total RNA was separated on a 1.2% formaldehyde/agarose gel and then transferred to a hybond XL membrane (GE Healthcare). The membrane was then cross-linked and probed with γ-$^{32}$P-labeled oligonucleotides (IDT1073 for the intron and IDT4685 for the mRNA, Supplementary Table S2) in Rapid-hyb buffer (GE Healthcare). The membrane was exposed on a phosphor screen and scanned on a Typhoon Trio. The images were quantified using ImageQuant.

### Western blot

Western blot analysis of LtrB relaxase was performed as previously described (17). Briefly, total cell lysate was separated on a 12% SDS-polyacrylamide gel and then transferred to 0.2 μM immuno-blot PVDF membrane (Bio-Rad). The membrane was blocked with 5% milk in TBS-T (20 mM Tris–HCl (pH 7.5), 140 mM NaCl, 2% Tween

20), incubated for 1 h with a 1/2,000 dilution of primary anti-relaxase antibody (gift from Gary Dunny, University of Minnesota), washed with TBS-T and incubated for 1 h with a 1/10 000 dilution of secondary HRP-labeled anti-rabbit antibody (Advansta). The imaging was done using chemiluminescent HRP substrate (Advansta WesternBright ECL) under a Bio-Rad ChemiDoc MP. For normalization, total protein from a Coomassie-stained 12% SDS-polyacrylamide gel was used as loading reference. Quantitation was done using Image Lab (Bio-Rad) software. For analysis of the IEP, after the 3-h induction, the same procedures were followed except that an anti-IEP antibody (Covance) was used as the primary antibody.

### mRNA degradation

For the pCY20 constructs, cells were grown at 30°C to $OD_{600}$ 0.5, temperature-shifted and induced with nisin for 1 h before adding rifampicin to a final concentration of 0.2 mg/ml. For the pRS01 construct, cells were grown to $OD_{600}$ 0.3, temperature-shifted and grown for an additional 2 h before adding rifampicin to a final concentration of 0.2 mg/ml. The cells were collected immediately at the end of each timepoint for analysis.

### RT-PCR

cDNA synthesis and amplification were performed using One*Taq* RT-PCR Kit (New England Biolabs) following the manufacturer's instructions. Briefly, 500 ng of DNase (Promega RQ1 DNase)-treated total RNA was used in a 20 μl first-strand synthesis reaction utilizing the randomized primer mix. Control reactions without reverse transcriptase added (RT-) were also performed. The first-strand synthesis reactions were then diluted to 50 μl, from which 2 μl was used for PCR amplification. The PCR reactions were performed utilizing specific primers (Supplementary Table S3) with the following conditions: 95°C for 30 s, (94°C for 20 s, 56°C for 30 s, 68°C for 15 s) × 27–32 cycles (individually optimized for each amplicon) and 68°C for 5 min. The amplicons were analyzed on 1% agarose gels.

### Construction of pCY20 LtrB::Ll.LtrB ΔORF plasmid

To delete the ORF from DIVb of the Ll.LtrB intron in the pCY20 LtrB::Ll.LtrB plasmid (Supplementary Table S1), oligonucleotide primers IDT6858 and IDT6859 (Supplementary Table S2), each containing an MluI endonuclease restriction site, were used to amplify the sequence flanking the ORF using CloneAmp HiFi PCR kit (Takara). The ∼12 kb PCR fragment was then digested with MluI (New England Biolabs) and ligated using T4 DNA ligase (New England Biolabs). The precise ORF deletion was verified by sequencing (EtonBio).

### pRS01 conjugation

An approach similar to that previously reported (17) was used to test conjugation frequency for the inducible constructs, except that the donor cells were preincubated in cold before the overnight mating. Briefly, fusidic acid-resistant *L. lactis* IL1403 ($FA^R$) was used as the recipient. *L. lactis* IL1403 pRS01 LtrB::tet ($Erm^R$) with its *ltrB* gene interrupted was used as the donor, which also contained either the intronless plasmid pCY20 LtrB, or the intron-containing plasmid pCY20 LtrB::Ll.LtrB (Supplementary Table S1). The donors and the recipient were grown to an $OD_{600}$ of 0.5–0.6 and subjected to temperature shift. Nisin was added to a final concentration of 0.4 μg/ml and the cells were incubated at appropriate temperatures for 3 h. The recipient was grown for an additional 3 h. Equal amounts of donor and recipient cells were mixed at the end of the 3-h induction, collected by centrifugation and resuspended in fresh GM17 media to remove the nisin. The nisin-free resuspended cells were spotted on filters (0.45 μm pore size, Millipore) on GM17 plates, and incubated for 18 h at 30°C. The filters were washed with 5 ml GM17 in a 50 ml conical tube by vortexing. The wash was then spotted or plated for single colonies on GM17 plates containing 25 μg/ml FA and 10 μg/ml Erm for selection of transconjugants. Plates were incubated for 18 h at 30°C. To calculate the number of input donor, the donor strain was plated on GM17 containing 10 μg/ml erythromycin. Conjugation frequency was calculated as exconjugants per donor ($Erm^R FA^R/Erm^R$).

For the native-donor conjugation experiment, *L. lactis* IL1403 pRS01 and *L. lactis* IL1403 ($FA^R$) were used as donor and recipient strains for conjugation, respectively. The donor cells were grown to an $OD_{600}$ of 0.5–0.6 and were subjected to temperature shift and continued incubation at appropriate temperatures for 3 h or 6 h. The conjugation rate was calculated in the same way as the induced construct.

## RESULTS

### Group II intron splicing *in vivo* is inhibited at low temperatures

Using an inducible expression construct, pCY20 (Supplementary Table S1) (17,21), we probed changes in the splicing of the Ll.LtrB intron upon exposure to various stressors that are commonly encountered by *L. lactis*. Among anaerobic and aerobic growth, glucose starvation, high and low temperatures, osmotic stress, copper, log phase growth and UV irradiation conditions, low temperature (10°C) in particular was striking in its inhibition of *in vivo* splicing efficiency (Figure 2A). The extent of the inhibition *in vivo* at 10°C was reproducibly between 75% and 90% (Figure 2B–D). We further expanded this experiment and determined that such temperature effects begin at 17°C (Figure 2C), with 10°C yielding the lowest splicing efficiency among all temperatures tested (Figure 2B and D). At 10°C, cell growth still occurs, albeit to a much lower extent (22). As a result of the cold shock, both levels of the induced intron RNA and the IEP were significantly lower (Figure 2C and Supplementary Figure S1A). Paradoxically, the mRNA level in cold was not only maintained but even increased with time (Figure 2C), despite the low levels of transcription and splicing (to be discussed later).

To test if such results are reproducible using different expression systems, we employed a constitutive expression construct pDL278 (Supplementary Table S1) (17,23),

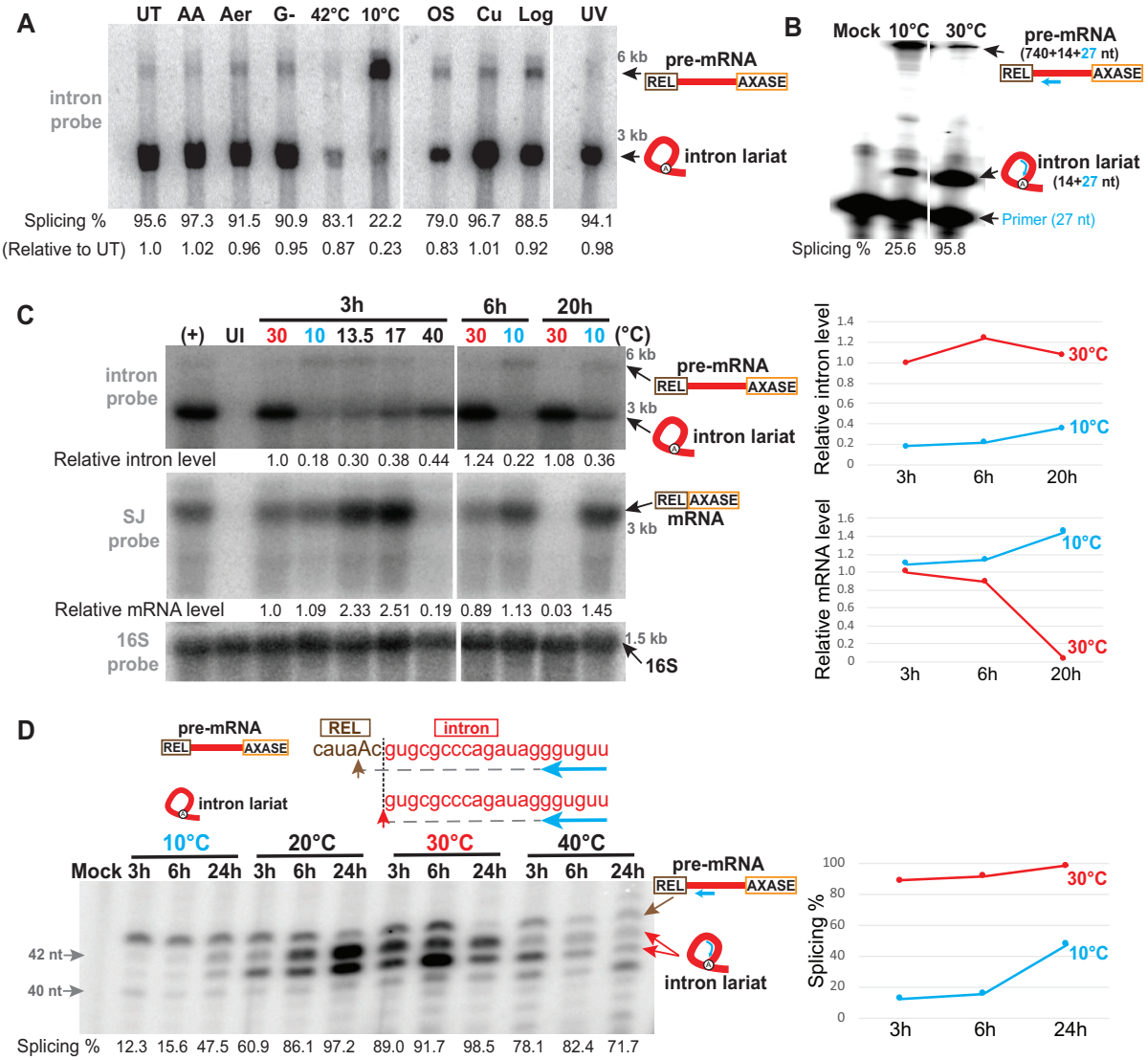


**Figure 2.** Splicing of the Ll.LtrB intron is inhibited *in vivo* in the cold. (**A**) Cold shock selectively inhibits group II intron splicing *in vivo*. The Ll.LtrB intron RNA expressed from the pCY20 plasmid with nisin induction and under stress was examined by northern blot using an intron-specific probe. UT: untreated control; AA: anaerobic growth; Aer: aerobic growth; G-: glucose deprivation; 42°C and 10°C: growth at specified temperatures; OS: osmotic stress; Cu: growth in the presence of copper ion; Log: induction of expression in log phase; UV: UV irradiation. Products were separated on an agarose/formaldehyde gel before blotting. The splicing efficiency (Splicing %) listed under each lane is defined as the amount of spliced intron divided by the sum of the amounts of spliced intron and the unspliced pre-mRNA. The relative values to the untreated control are also listed. (**B**) Splicing efficiency of the intron is reduced under cold shock. Primer extension results compare splicing at 10°C and 30°C for 3 h. The oligonucleotide primer is 14 nt away from the 5′ of the intron. Primer extension products were resolved on an 8% urea/polyacrylamide gel. 'Mock' denotes the same reaction without RNA added. Splicing % is listed under each lane. (**C**) Northern blot showing levels of mRNA and intron at different temperatures and times. A splice junction (SJ) probe, an intron probe and a 16S rRNA probe were used to show the levels of mRNA, intron and 16S rRNA, respectively. The experiment was as described in panel A. '+' denotes a spliced intron as the positive control. 'UI' denotes sample from uninduced cells. Relative mRNA levels were normalized to 16S rRNA. Relative intron levels were calculated based on the sum of the precursor and the spliced intron and normalized to 16S rRNA. Plots for relative levels of the intron and the mRNA at 10°C and 30°C are shown on the right. (**D**) Temperature effects on *in vivo* splicing. Primer extension termination assay was used with addition of ddTTP to the same primer extension reaction as in panel B. This resulted in a 1–2 nt difference in cDNA lengths for the precursor and spliced product. Cells were grown at four different temperatures for 3, 6 or 24 h before analysis. Products of the primer extension were resolved on a 6% urea/polyacrylamide sequencing gel. Two bands are routinely observed corresponding to the intron lariat (red arrow). Splicing % listed below the gel images is defined as the amount of spliced intron (lower two bands) divided by all three bands indicated. Splicing % at 10°C and 30°C are plotted on the right.

with which we observed similar inhibition of splicing after downshifting the temperature (Supplementary Figure S1B). Therefore, splicing inhibition of the group II intron at low temperatures is not an artefact related to the nisin-inducible promoter from the pCY20 plasmid.

According to minor structural variations, group II introns are classified into three subgroups IIA, IIB and IIC, and Ll.LtrB belongs to the IIA group. To test whether such cold-inhibition of splicing is a characteristic of other types of group II introns as well, we expressed a group IIB intron (EcI5, from *E. coli*) (24) and a IIC intron (BhI1, from *Bacillus halodurans*) (25) (Supplementary Table S1) in *E. coli* MC1061 at 10°C, 20°C, 30°C and 37°C. We observed similar splicing inhibition effects upon temperature downshift (under 20°C) (Supplementary Figure S2). It is thus likely that low-temperature sensitivity *in vivo* is a common feature of bacterial group II introns.

## Cold abolishes Ll.LtrB self-splicing

To investigate the cold sensitivity of the RNA without the influence of the IEP, we employed intron RNA synthesized *in vitro* and subjected it to self-splicing conditions (26). Splicing was measured within the 10°C - 40°C temperature range after a 3-h incubation. The self-splicing efficiency was temperature-dependent, with 40°C and 30°C having the largest proportion of intron RNA spliced (Figure 3A, 85.4% and 57.3%, respectively). Interestingly, whereas the 20°C treatment allowed a small amount of splicing to occur (3.7%), at 10°C the self-splicing was completely abolished even after a 24-h incubation (Figure 3A and B), implying that splicing was halted rather than occurring at a slower rate. Upon raising the temperature from 10°C to 30°C, the splicing inhibition was relieved (Figure 3C), suggesting that a thermal barrier prevented the ribozyme at 10°C from becoming catalytically active.

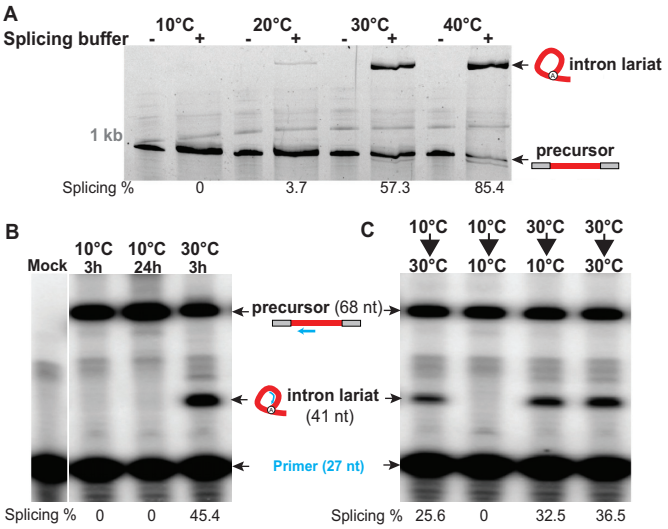


**Figure 3.** Ll.LtrB intron self-splicing *in vitro* is abolished in the cold. (**A**) Inhibition of self-splicing with a 3-h incubation at 10°C. The *in vitro*-transcribed intron precursor was subjected to self-splicing in a buffer supplemented with 50 mM $Mg^{2+}$ at 10°C, 20°C, 30°C and 40°C for 3 h and resolved on an 8% urea/polyacrylamide gel followed by SYBR Green staining. Lariat RNA migrates slowly on this gel type. (**B**) Splicing inhibition with extended incubation. The intron RNA subjected to self-splicing at 10°C and 30°C for 3 or 24 h was analyzed by primer extension as in Figure 2B. Primer extension products were resolved by 8% urea/polyacrylamide gel. 'Mock' denotes the same reaction without RNA added. Splicing % listed under each lane is defined as the spliced intron divided by the sum of the spliced intron and the precursor. (**C**) Reversibility of cold temperature effects on intron self-splicing. The intron RNA was subjected to self-splicing initially at one temperature for 1 h and then for an additional 1 h at the same temperature or a different one as indicated, after which the RNA was analyzed by primer extension as in Figure 2B.

## Cold sensitivity can be rescued by the IEP

The discrepancy in the extent of the splicing inhibition by cold between *in vivo* (~10–25% splicing) and *in vitro* results (no self-splicing) prompted us to investigate the IEP's role in splicing under cold stress. We therefore carried out *in vitro* splicing assays with physiological buffering conditions in the presence of excess IEP purified from *E. coli* (19) at 10–40°C. Interestingly, at 10°C, in contrast to self-splicing conditions, a small portion of the intron was spliced with the help of the IEP after a 3-h incubation (Figure 4A, 5.9% splicing). Splicing was high at 20°C and 30°C (62.4% and 47.9%, respectively), whereas at 40°C there was barely any splicing (2.1%), likely because the IEP is inactivated (Figure 4A) (27). Binding of the IEP to the intron RNA in cold appeared within a normal range as shown by gel-shift assay (Supplementary Figure S3). Interestingly, with an extended incubation at 10°C (24 h), the IEP-assisted splicing was restored to almost the level of that treated at 30°C for 3 h (Figure 4B, 38.6% versus 41.3%). Thus, in the cold, the IEP alleviates the splicing inhibition and enables splicing, albeit at a lower rate.

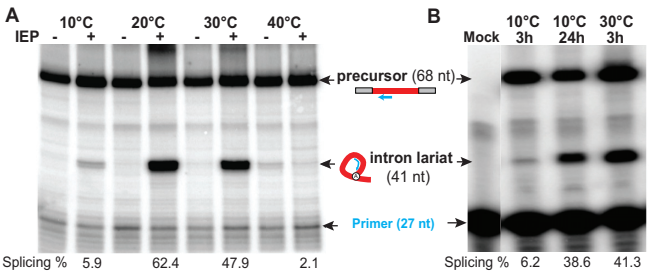


**Figure 4.** Splicing of Ll.LtrB intron in the cold is rescued by the IEP. (**A**) IEP-assisted *in vitro* splicing of the intron at different temperatures. The *in vitro*-transcribed intron precursor RNA was subjected to splicing in a buffer supplemented with 5 mM $Mg^{2+}$ in the presence (+) or absence (–) of excess IEP at 10°C, 20°C, 30°C and 40°C for 3 h and analyzed by primer extension as in Figure 2B. (**B**) Recovery of IEP-assisted intron splicing by 24-h incubation. The *in vitro*-transcribed intron precursor RNA subjected to splicing at 10°C for 3 and 24 h was compared to that at 30°C for 3 h. Splicing reactions were analyzed by primer extension as described in Figure 2B.

## Splicing inhibition is attributed to disrupted RNA folding in cold

We next sought to determine the cause of splicing inhibition within the intron RNA. Inspired by various examples of RNA thermometers, which react to temperature shifts by changing their secondary and/or tertiary structures (28,29),

we probed whether the folding of the intron RNA is affected by the low temperature.

We used selective 2′-hydroxyl acylation analyzed by primer extension (SHAPE) to probe the RNA *in vitro* in the presence and absence of the IEP at 10°C and 30°C (Supplementary Figure S4). The majority of the nucleotides at 10°C share the same modification profile as at 30°C, indicative of well-formed RNA secondary structures (Figure 5A). However, the 10°C SHAPE profile for nucleotides involved in some tertiary structures exhibited substantial changes. Particularly, nucleotides in DI involved in α–α′ and β–β′ interactions showed increased SHAPE reactivity (Figure 5A), suggesting disengagement of those two structurally essential tertiary interactions, which would disrupt the folding between the two halves of DI (30) (Figure 5B). The results also indicated that in cold, the nucleotides in DV involving the catalytic triad, κ′ and μ′ undergo extensive SHAPE reactivity changes, indicative of a disrupted structure at the center of the active site (Figure 5), which would explain the inability to splice. Although we did not observe changes at the junction of DII and DIII (J2/3), which forms part of the active site, SHAPE changes were exhibited in adjacent nucleotides. DII and DIII exhibited altered SHAPE profiles in cold as well, with DIII having increased flexibility at nucleotides in the DV-interacting μ motif (Figure 5). Moreover, nucleotides at and near the 5′ end of the intron exhibit strong SHAPE modifications, indicative of disturbance of the first step of splicing.

The structure profiles of intron RNAs under self-splicing conditions were also investigated, showing generally similar results as those for the IEP-assisted counterparts. Exceptions, like nucleotides in the α motif, where different SHAPE profiles were revealed, are possibly due to increased RNA stacking in the high-salt environment (Supplementary Figure S5).

### Cold effects on relaxase gene expression

Within its native conjugative plasmid pRS01, the Ll.LtrB intron interrupts the *ltrB* gene (18). It was previously demonstrated that the Ll.LtrB intron targets and reduces levels of the mRNA from which it was spliced to a very low level, by a spliced-exon reopening (SER) reaction (17). We therefore carefully examined the relaxase mRNA level after cold treatment. Interestingly, despite both transcription and splicing being inhibited at low temperature, which resulted in a substantial reduction in level of the spliced intron, the mRNA level was maintained and even increased with time compared to 30°C (Figure 2C and Supplementary Figure S6A). Consistent with this paradoxical finding, which is in accord with destructive mRNA targeting by the intron (17), relaxase levels measured by Western Blot showed that at 10°C the relaxase level matched that at 30°C after a 3-h induction (Supplementary Figure S6B). This result suggests that a mechanism exists for maintaining relaxase levels in the context of a global decrease in translation (31). Since a similar construct that does not contain the intron also showed increased mRNA and relaxase levels in cold (Supplementary Figure S6A and B), high mRNA levels upon cold shock is unlikely due exclusively to the influence of the intron. Moreover, the build-up of mRNA over a longer time-course was also demonstrated by the constitutive construct pDL278 (Supplementary Figure S6C), indicating that inducible expression is not the cause of *ltrB* mRNA accumulation under cold shock.

To discern the intron's role in the maintenance of relaxase mRNA levels in the cold, we measured mRNA turnover after rifampicin treatment, utilizing the pCY20 constructs with and without the intron present (Figure 6A). The results showed that the mRNA expressed from the intronless construct degraded at a slower rate in the cold, with a half-life of 81 min at 10°C versus 33 min at 30°C. Surprisingly, levels of spliced mRNA expressed from the intron-containing construct actually increased with time at 10°C, likely reflecting low levels of splicing, which ensures a supply of mRNA in the cold (Figure 6A and B).

In addition, to compare relaxase mRNA levels to other cellular RNAs in the cold, we performed RT-PCR on messages transcribed from the pRS01 plasmid (*ltrM*, *ltrC*, *ltrE*, *ltrF*, *virD4* and *cluA*), as well as from bacterial genomic loci (cold shock-related genes *cspE* and *cspB*, heat shock-related gene *groES* and house-keeping genes *copA* and *gyrB*) (Supplementary Figure S7A). The results showed that most genes, including house-keeping genes and those transcribed from pRS01, had higher levels of mRNA at 10°C than at 30°C, as for relaxase mRNA. As controls, cold-shock protein mRNAs *cspE* and *cspB* were dramatically upregulated in cold, whereas the heat shock-related *groES* mRNA was higher at 30°C than at 10°C (Supplementary Figure S7A). Furthermore, RT-PCR after rifampicin-treatment showed that except for heat-shock *groES* mRNA, messages degraded more slowly in cold (Supplementary Figure S7B), consistent with the notion that stability of prokaryotic mRNAs increases under stress (32–35). Taken together, under cold stress, slow intron splicing, reduced mRNA-targeting by the intron, as well as decreased RNA degradation all contribute to relaxase mRNA maintenance.

### Cold effects on retromobility and horizontal transfer of the Ll.LtrB intron

To investigate the retromobility of the intron under cold stress, we tested the retrotransposition frequency using methods described previously (36). As expected, we observed significantly reduced retrotransposition activity (∼30-fold decrease, data not shown), indicative of both reduced expression and mobility of the group II intron within the host cell at temperatures <20°C.

Because the LtrB relaxase is essential for conjugal transfer of the Ll.LtrB intron's host plasmid pRS01, we next investigated the impact of cold on conjugation. The native pRS01 construct, which constitutively expressed relaxase, served as the conjugal donor ($Erm^R$), and was incubated at 10°C for 3 or 6 h before mating with the recipient cells ($FA^R$) overnight at 30°C. The number of exconjugants ($Erm^R$ $FA^R$) showed that whereas the 3-h treatment resulted in a slightly lower conjugation frequency compared to 30°C, a 6-h cold treatment yielded a conjugation frequency that was 4-fold higher than the cells treated at 30°C (Supplementary Figure S8A). This likely correlates to the levels of available mRNA upon mating (Supplementary Figure S7A), as paralleled by the mRNA levels of the constitutively overex-

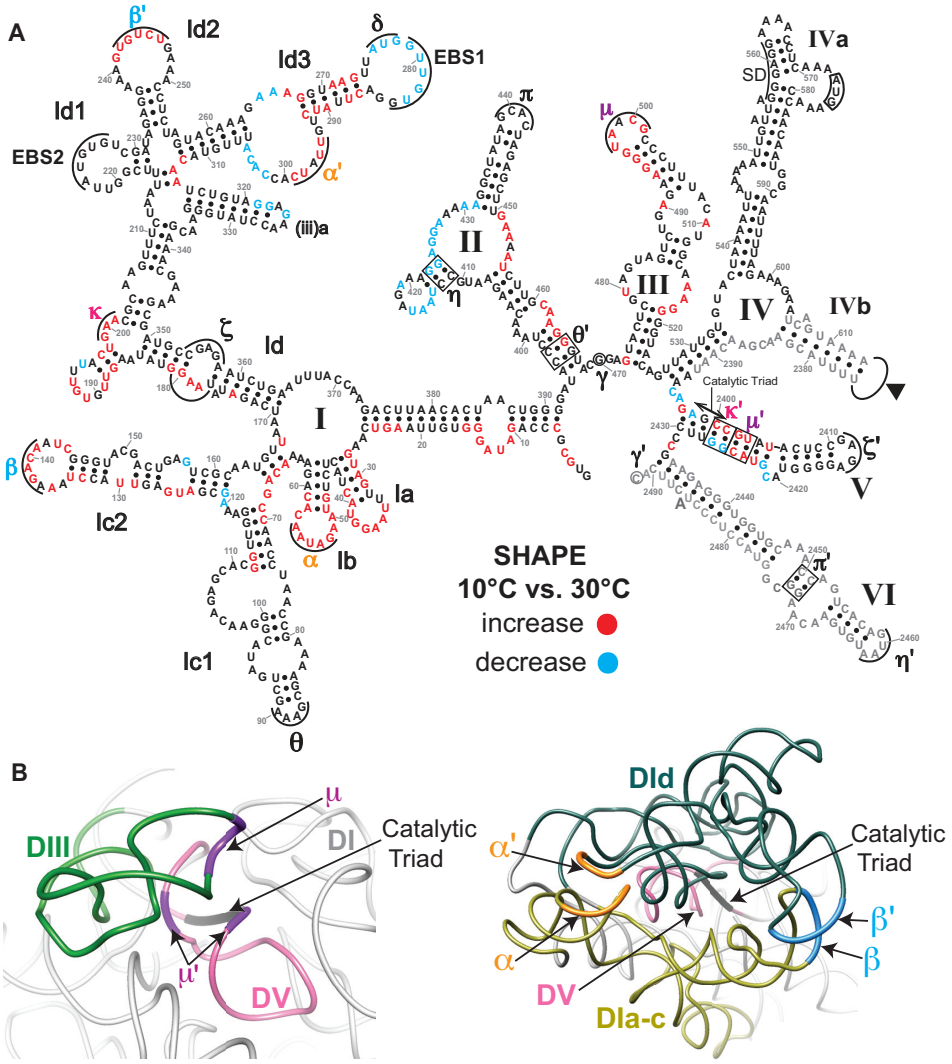


**Figure 5.** SHAPE profiling reveals intron structure disruptions under cold shock. (**A**) Superimposed SHAPE profile representing overall differences between the 10°C and 30°C samples. SHAPE modifications were analyzed by primer extension on a 6% urea/polyacrylamide sequencing gel (Supplementary Figure S4). SHAPE profiling was performed on the intron RNA subjected to IEP-assisted *in vitro* splicing at 10°C or 30°C for 3h. Differences in SHAPE profiles comparing 10°C to 30°C are highlighted in colors (red denotes increased SHAPE reactivity in cold and blue denotes decreases). Nucleotides shown in grey were excluded from SHAPE probing. (**B**) 3D illustration of important tertiary interactions displayed in panel A as shown in cryo-EM structure of the intron RNP (PDB: 5g2x) (12). Left: DIII locks DV (pink) into DI primarily via the μ–μ′ (purple) interaction. Right: DIa-c (yellow) makes contact with the distal DId (teal) primarily via α–α′ (orange) and β–β′ (blue) interactions, forming the essential DI scaffold. The catalytic triad nucleotides are denoted by enlarged black tubes.

pressed construct treated in a similar fashion (the pDL278 construct, Supplementary Figure S6C). This elevated level of conjugation could be attributed both to increased transcription or mRNA stability over time and to the paradoxical increase of mRNA caused by lower intron levels (Figure 2C and Supplementary Figures S6C and S7B).

To rule out the role of any pre-accumulated relaxase mRNA and protein prior to induction, we also tested pRS01 with inactivated relaxase, which was instead provided *in trans* by the inducible pCY20 constructs used previously (17). The results showed that a 3-h induction at 10°C yielded a similar conjugation frequency to 30°C (Figure 6C and D), consistent with the levels of the mRNA and protein at the beginning of the conjugation period (Figure 2C and Supplementary Figure S6A and B). In addition, conjugation frequencies of the same construct without the intron at both temperatures showed similar results (Supplementary Figure S8B), consistent with their mRNA and relaxase levels (Supplementary Figure S6A and B), suggesting a similar general effect on relaxase gene expression as described above, in addition to influences imposed by the intron. In contrast, the same intron-containing construct with the IEP ORF deleted (ΔORF) or in which relaxase was not induced exhibited no conjugation activity in the absence of the IEP (Figure 6C and D). These results not only argue against leaky nisin-induced expression after incubation in the cold, but also underscore the paramount role in splicing of the IEP, which is required for host conjugative relaxase

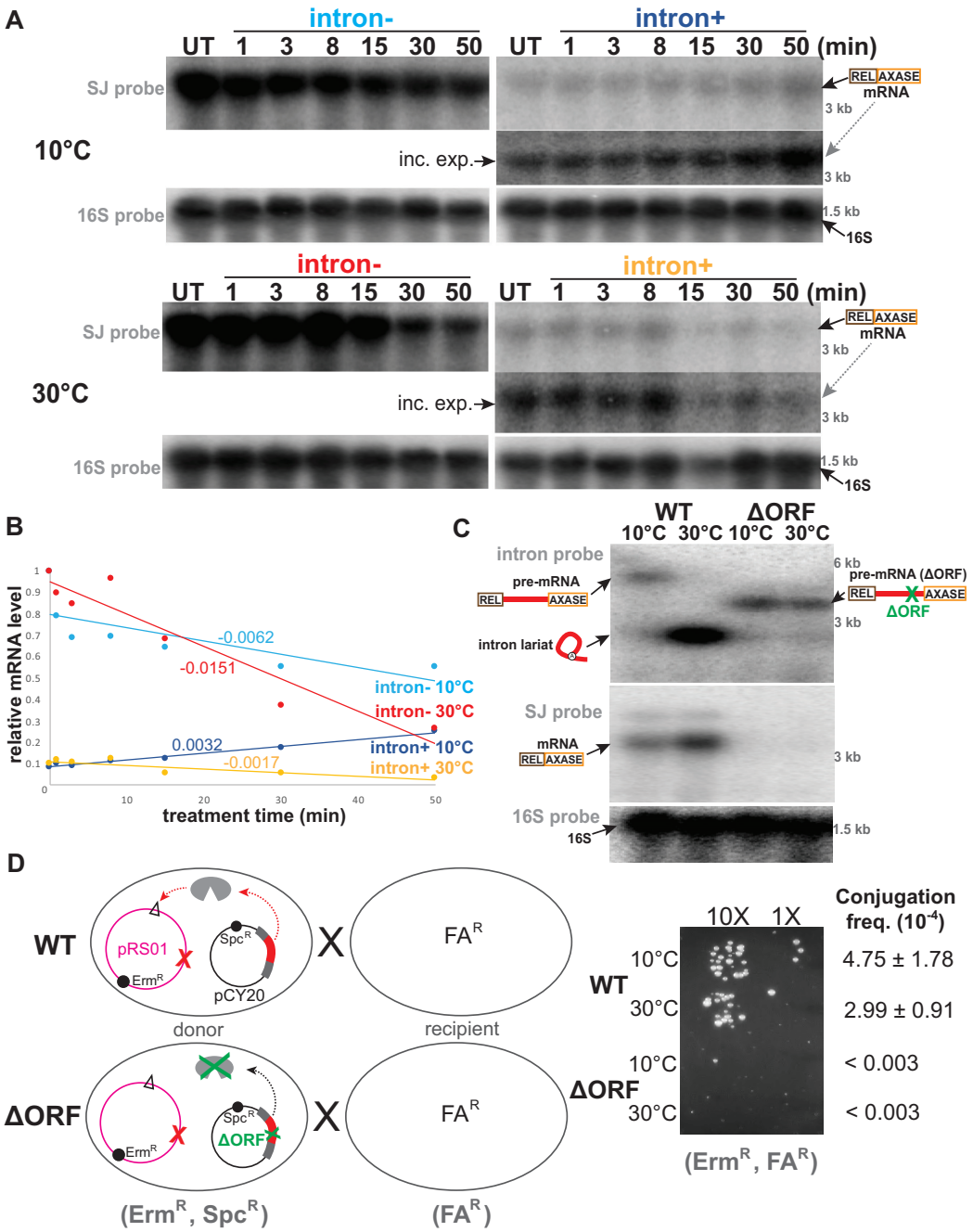


**Figure 6.** Host relaxase expression and pRS01 conjugative transfer in the cold. (**A**) Relaxase mRNA turnover. Northern blot shows relaxase mRNA levels in the pCY20 constructs (intron+ and intron–) after rifampicin treatment for up to 50 min at 10°C and 30°C. Cells were grown to $OD_{600}$ 0.5 at 30°C and shifted to 10°C or 30°C, followed by nisin induction for 1 h before rifampicin treatment. The RNA was analyzed using the splice junction (SJ) probe and the 16S rRNA probe as in Figure 2C. (**B**) Quantitation of the Northern blot results in panel A. Relaxase mRNA levels were normalized to 16S rRNA and plotted against time of rifampicin treatment. The slopes are indicated. Color code is the same as in panel A. (**C**) Deletion of the IEP ORF abolishes splicing and mRNA production. Northern blot results showing the intron RNA and mRNA levels for WT and ΔORF constructs at 10°C and 30°C. (**D**) Conjugation frequency of the pRS01 plasmid with relaxase (grey) provided *in trans*. The pRS01 plasmid (pink circle) is relaxase-minus (LtrB::Tet, as indicated by red cross). Relaxase was instead provided from the pCY20 plasmid (black circle) with (WT) or without (ΔORF) IEP expressed from a nisin-inducible promoter under cold shock. The origin of conjugation is denoted by the triangle. A separate experiment using uninduced WT donor cells at both 10°C and 30°C was done and yielded conjugation frequencies of less than $0.003 \times 10^{-4}$ (data not shown). Exconjugants were counted on plates with single $Erm^R$ $FA^R$ colonies. The conjugation frequency for the WT and ΔORF constructs was calculated from results of six and three experiments, respectively. Spot tests (non-quantitative) on same media are shown to the right.

expression and subsequent horizontal plasmid-plus-intron transfer.

## DISCUSSION

### Thermosensing RNAs as genetic regulators

Among macromolecules, RNAs are distinctive for their structural versatility in varying thermal conditions. Temperature-sensitive non-coding RNAs, called RNA thermometers, are often used by cells to regulate genes required during either a heat shock or cold shock response (29,37). Moreover, temperature shifts have been shown to induce transcriptome-wide RNA structural changes, which may be of regulatory significance (38,39). In the current work, we found that the splicing of the group II intron Ll.LtrB was inhibited at low temperatures, and that such cold sensitivity is also shared by other classes of bacterial group II introns. It is therefore interesting to consider group II introns as RNA thermosensors that at low temperatures have disrupted higher-order structures, which can be restored upon temperature upshift (Figure 3C). These properties are similar to *cspA* mRNA, which is a thermosensor that regulates translation of cold-shock protein CspA (40).

### Reasons for cold sensitivity of group II intron splicing

Unlike most large, well-structured RNAs such as group I introns, group II introns are known to have a smooth folding landscape, with the tertiary interactions forming with the assistance of DI to allow the RNA to achieve its native state (7,41). A disrupted active site, which normally forms at DV, is likely the direct cause of the inability to splice at low temperatures. Whereas most secondary structures seem to form properly during transcription in the cold, the failure to form key tertiary interactions, including α–α′ and β–β′ (Figures 1B and 5 and Supplementary Figure S4), would prevent formation of the native conformation of the entire DI (Figures 1B and 5B), which has a central role in the correct folding of group II introns (5,42). Also, increased SHAPE reactivity in the κ–ζ region (Figure 5A and Supplementary Figure S4) may result in unsuccessful tertiary collapse of DI, attributable to a kinetic trap formed around the κ–ζ region, proper folding of which is essential for maturation of the entire ribozyme (8,43). Further, the disruption of the κ–κ′ and μ–μ′ interactions (Figure 5) likely contribute to the misdocking of DV at the core of the active site.

It is also likely that the RNA would tend to be less flexible in cold due to decreased thermally dependent movements, making it difficult for tertiary interactions to form. Then, the IEP could facilitate establishment of tertiary contacts that are required for RNP structure and RNA catalysis (3,44), as suggested by the ability of the IEP to rescue group II intron splicing at cold temperatures (Figure 4). Conversely, cold may negatively impact RNA–protein interactions, as the subdomains DIc2 and DId2 joined by β–β′, interact with the thumb domain of the IEP (Figures 1B and 5) (12). Regardless, the cold-sensitivity is inherent to the RNA, as demonstrated by the lack of self-splicing at low temperature. In the cell, molecular chaperones such as cold-shock proteins (45) may influence both the intron RNA and the IEP, which could explain the elevated splicing efficiency *in vivo* compared to IEP-assisted splicing *in vitro* (Figures 2 and 4A).

### Evolutionary implication of IEP-mediated thermal rescue

Coevolution of group II introns and IEPs has been proposed based on structural characteristics (46). Although numerous group II introns have been shown to splice better at high temperature *in vitro* (25,47), splicing conditions involving the IEP or in-cell scenarios have not been adequately addressed. Our data suggest that it is advantageous for group II intron RNAs to have protein partners in the context of unfavorable and changing environments, in particular, temperature downshifts. In an RNA world, it would have been disadvantageous for the primitive introns to have impaired splicing in rapidly changing thermal conditions. Our results suggest that the advent of protein partners would have allowed the RNA to adapt to a wider range of temperatures, thus obtaining a significant advantage in evolution. The IEP is also capable of assisting splicing of a cognate group II intron when co-expressed in non-native hosts (26,48), which often live at different ambient temperatures. Such protein-mediated effects could potentially facilitate the adaptation and spread of group II introns in non-native hosts. Taken together, RNP catalysis would seem advantageous over pure ribozyme reactivity (49), especially in shifting and unfavorable environments.

Temperature-regulated splicing may be a common feature shared by both group II introns and eukaryotic spliceosomes. For example, in mammals, alternative splicing of eukaryotic introns has been shown to change upon temperature shifts (50). In addition, temperature was shown to regulate splicing of the abovementioned cold-inducible RNA-binding protein gene *Cirbp* in mammalian cells (51). It is thus possible that such temperature-sensing is a vestige from the RNA world, with some of the more subtle roles of sensing delegated to protein factors, which together co-evolved into the spliceosome.

### Cold-sensing, host gene regulation, conjugation and mobility of group II introns

Bacteria are known to exhibit a dynamic transcriptome upon exposure to stress conditions (52,53). In this study we observed altered levels of the spliced intron RNA and mRNA *in vivo* in response to cold stress. The reduction in intron levels could be attributed to downregulated transcription in cold shock as well as to splicing inhibition. However, the maintenance or build-up of mRNA is more nuanced, considering that its production relies on transcription and splicing on one hand, and on decreased levels of cellular RNA decay that is facilitated and enhanced by the targeting of the mRNA by the intron on the other (17). Thus, the relatively high level of mRNA under cold stress is accounted for by both general decrease in cellular mRNA decay and low levels of the intron due to splicing inhibition, with a resulting reduction in SER (mRNA targeting). In addition to the reduced SER, the retarded splicing may also result in increased stability of the relaxase mRNA by preventing rapid mRNA build-up, which could trigger increased degradation

(54). Splicing of the intron may thus not only serve as an additional layer of post-transcriptional regulation, but also fine-tune relaxase gene expression under cold stress, to help promote conjugation, thereby aiding bacteria as they adapt to fluctuating environments (32,34,54).

Although such regulation may be counterintuitive, the maintenance of conjugation, which results from increased relaxase mRNA levels, is actually in accord with both the conjugative plasmid and its resident group II intron as 'selfish' elements. As a general rule, transferring to a new host, whose integrity is not threatened, is considered favorable for selfish mobile elements (55) including conjugative plasmids (56–58). Since retromobility, one of the two ways for the Ll.LtrB intron to spread and thrive, is inhibited under cold stress (data not shown), the intron may benefit from conjugal transfer, by maintaining mRNA and therefore relaxase levels. Thus, by promoting horizontal transfer of the conjugative plasmid, the intron can piggy-back into a new host. Collaboration between conjugative and retrotransposable elements to promote horizontal transfer has been previously reported, whereby group II intron splicing generates relaxase for conjugation, whereas relaxase introduces DNA nicks that facilitate retrotransposition (15). As an extension of such collaboration between mobile elements, by functioning as a thermosensor of cold shock, the intron helps achieve not only spread of the conjugative plasmid on which it resides, but also its own survival.

## SUPPLEMENTARY DATA

Supplementary Data are available at NAR Online.

## ACKNOWLEDGEMENTS

We thank Olga Novikova, Justin Waldern and Jake Bailey for discussions and comments on the manuscript.

## FUNDING

National Institutes of Health (NIH) [GM39422, GM44844 to M.B.]; G.Q. was supported by the Advanced Talents Incubation Program of Hebei University (start-up grant to G.Q.); National Natural Science Foundation of China (NSFC) [31971227 to G.Q.]. The open access publication charge for this paper has been waived by Oxford University Press – *NAR* Editorial Board members are entitled to one free paper per year in recognition of their work on behalf of the journal.

*Conflict of interest statement.* None declared.

## REFERENCES

1. Lambowitz,A.M. and Zimmerly,S. (2011) Group II introns: mobile ribozymes that invade DNA. *Cold Spring Harb. Perspect. Biol.*, **3**, a003616.
2. Lambowitz,A.M. and Belfort,M. (2015) Mobile bacterial group II introns at the crux of eukaryotic evolution. *Microbiol Spectr*, **3**, doi:10.1128/microbiolspec.MDNA3-0050-2014.
3. Noah,J.W. and Lambowitz,A.M. (2003) Effects of maturase binding and Mg2+ concentration on group II intron RNA folding investigated by UV cross-linking. *Biochemistry*, **42**, 12466–12480.
4. Dong,X., Ranganathan,S., Qu,G., Piazza,C.L. and Belfort,M. (2018) Structural accommodations accompanying splicing of a group II intron RNP. *Nucleic Acids Res.*, **46**, 8542–8556.
5. Pyle,A.M. (2010) The tertiary structure of group II introns: implications for biological function and evolution. *Crit. Rev. Biochem. Mol. Biol.*, **45**, 215–232.
6. Su,L.J., Waldsich,C. and Pyle,A.M. (2005) An obligate intermediate along the slow folding pathway of a group II intron ribozyme. *Nucleic Acids Res.*, **33**, 6674–6687.
7. Waldsich,C. and Pyle,A.M. (2008) A kinetic intermediate that regulates proper folding of a group II intron RNA. *J. Mol. Biol.*, **375**, 572–580.
8. Donghi,D., Pechlaner,M., Finazzo,C., Knobloch,B. and Sigel,R.K. (2013) The structural stabilization of the kappa three-way junction by Mg(II) represents the first step in the folding of a group II intron. *Nucleic Acids Res.*, **41**, 2489–2504.
9. Chan,R.T., Peters,J.K., Robart,A.R., Wiryaman,T., Rajashankar,K.R. and Toor,N. (2018) Structural basis for the second step of group II intron splicing. *Nat. Commun.*, **9**, 4676.
10. Toor,N., Keating,K.S., Taylor,S.D. and Pyle,A.M. (2008) Crystal structure of a self-spliced group II intron. *Science*, **320**, 77–82.
11. Robart,A.R., Chan,R.T., Peters,J.K., Rajashankar,K.R. and Toor,N. (2014) Crystal structure of a eukaryotic group II intron lariat. *Nature*, **514**, 193–197.
12. Qu,G., Kaushal,P.S., Wang,J., Shigematsu,H., Piazza,C.L., Agrawal,R.K., Belfort,M. and Wang,H.W. (2016) Structure of a group II intron in complex with its reverse transcriptase. *Nat. Struct. Mol. Biol.*, **23**, 549–557.
13. Costa,M., Walbott,H., Monachello,D., Westhof,E. and Michel,F. (2016) Crystal structures of a group II intron lariat primed for reverse splicing. *Science*, **354**, aaf9258.
14. Haack,D.B., Yan,X., Zhang,C., Hingey,J., Lyumkis,D., Baker,T.S. and Toor,N. (2019) Cryo-EM structures of a group II intron reverse splicing into DNA. *Cell*, **178**, 612–623.
15. Novikova,O., Smith,D., Hahn,I., Beauregard,A. and Belfort,M. (2014) Interaction between conjugative and retrotransposable elements in horizontal gene transfer. *PLos Genet.*, **10**, e1004853.
16. Novikova,O. and Belfort,M. (2017) Mobile group II introns as ancestral eukaryotic elements. *Trends Genet.*, **33**, 773–783.
17. Qu,G., Piazza,C.L., Smith,D. and Belfort,M. (2018) Group II intron inhibits conjugative relaxase expression in bacteria by mRNA targeting. *Elife*, **7**, e34268.
18. Mills,D.A., McKay,L.L. and Dunny,G.M. (1996) Splicing of a group II intron involved in the conjugative transfer of pRS01 in lactococci. *J. Bacteriol.*, **178**, 3531–3538.
19. Saldanha,R., Chen,B., Wank,H., Matsuura,M., Edwards,J. and Lambowitz,A.M. (1999) RNA and protein catalysis in group II intron splicing and mobility reactions using purified components. *Biochemistry*, **38**, 9069–9083.
20. Contreras,L.M., Huang,T., Piazza,C.L., Smith,D., Qu,G., Gelderman,G., Potratz,J.P., Russell,R. and Belfort,M. (2013) Group II intron-ribosome association protects intron RNA from degradation. *RNA*, **19**, 1497–1509.
21. Chen,Y., Staddon,J.H. and Dunny,G.M. (2007) Specificity determinants of conjugative DNA processing in the *Enterococcus faecalis* plasmid pCF10 and the *Lactococcus lactis* plasmid pRS01. *Mol. Microbiol.*, **63**, 1549–1564.
22. Panoff,J.M., Legrand,S., Thammavongs,B. and Boutibonnes,P. (1994) The cold shock response in *Lactococcus lactis* subsp. lactis. *Curr. Microbiol.*, **29**, 213–216.
23. LeBlanc,D.J., Lee,L.N. and Abu-Al-Jaibat,A. (1992) Molecular, genetic, and functional analysis of the basic replicon of pVA380-1, a plasmid of oral streptococcal origin. *Plasmid*, **28**, 130–145.
24. Zhuang,F., Karberg,M., Perutka,J. and Lambowitz,A.M. (2009) EcI5, a group IIB intron with high retrohoming frequency: DNA target site recognition and use in gene targeting. *RNA*, **15**, 432–449.
25. Toor,N., Robart,A.R., Christianson,J. and Zimmerly,S. (2006) Self-splicing of a group IIC intron: 5′ exon recognition and alternative 5′ splicing events implicate the stem-loop motif of a transcriptional terminator. *Nucleic Acids Res.*, **34**, 6461–6471.
26. Matsuura,M., Saldanha,R., Ma,H., Wank,H., Yang,J., Mohr,G., Cavanagh,S., Dunny,G.M., Belfort,M. and Lambowitz,A.M. (1997) A bacterial group II intron encoding reverse transcriptase, maturase, and DNA endonuclease activities: biochemical demonstration of maturase activity and insertion of new genetic information within the intron. *Genes Dev.*, **11**, 2910–2924.

27. Yao,J., Zhong,J., Fang,Y., Geisinger,E., Novick,R.P. and Lambowitz,A.M. (2006) Use of targetrons to disrupt essential and nonessential genes in *Staphylococcus aureus* reveals temperature sensitivity of Ll.LtrB group II intron splicing. *RNA*, **12**, 1271–1281.
28. Choi,E.K., Ulanowicz,K.A., Nguyen,Y.A.H., Frandsen,J.K. and Mitton-Fry,R.M. (2017) SHAPE analysis of the htrA RNA thermometer from *Salmonella enterica*. *RNA*, **23**, 1569–1581.
29. Kortmann,J. and Narberhaus,F. (2012) Bacterial RNA thermometers: molecular zippers and switches. *Nat. Rev. Microbiol.*, **10**, 255–265.
30. Zhao,C., Rajashankar,K.R., Marcia,M. and Pyle,A.M. (2015) Crystal structure of group II intron domain 1 reveals a template for RNA assembly. *Nat. Chem. Biol.*, **11**, 967–972.
31. Barria,C., Malecki,M. and Arraiano,C.M. (2013) Bacterial adaptation to cold. *Microbiology*, **159**, 2437–2443.
32. Redon,E., Loubiere,P. and Cocaign-Bousquet,M. (2005) Role of mRNA stability during genome-wide adaptation of *Lactococcus lactis* to carbon starvation. *J. Biol. Chem.*, **280**, 36380–36385.
33. Georgellis,D., Barlow,T., Arvidson,S. and von Gabain,A. (1993) Retarded RNA turnover in *Escherichia coli*: a means of maintaining gene expression during anaerobiosis. *Mol. Microbiol.*, **9**, 375–381.
34. Vargas-Blanco,D.A., Zhou,Y., Zamalloa,L.G., Antonelli,T. and Shell,S.S. (2019) mRNA degradation rates are coupled to metabolic status in *Mycobacteriumsmegmatis*. *mBio*, **10**, e00957-19.
35. Dressaire,C., Picard,F., Redon,E., Loubiere,P., Queinnec,I., Girbal,L. and Cocaign-Bousquet,M. (2013) Role of mRNA stability during bacterial adaptation. *PLoS One*, **8**, e59059.
36. Cousineau,B., Lawrence,S., Smith,D. and Belfort,M. (2000) Retrotransposition of a bacterial group II intron. *Nature*, **404**, 1018–1021.
37. Breaker,R.R. (2010) RNA switches out in the cold. *Mol. Cell*, **37**, 1–2.
38. Wan,Y., Qu,K., Ouyang,Z., Kertesz,M., Li,J., Tibshirani,R., Makino,D.L., Nutter,R.C., Segal,E. and Chang,H.Y. (2012) Genome-wide measurement of RNA folding energies. *Mol. Cell*, **48**, 169–181.
39. Chursov,A., Kopetzky,S.J., Leshchiner,I., Kondofersky,I., Theis,F.J., Frishman,D. and Shneider,A. (2012) Specific temperature-induced perturbations of secondary mRNA structures are associated with the cold-adapted temperature-sensitive phenotype of influenza A virus. *RNA Biol*, **9**, 1266–1274.
40. Giuliodori,A.M., Di Pietro,F., Marzi,S., Masquida,B., Wagner,R., Romby,P., Gualerzi,C.O. and Pon,C.L. (2010) The cspA mRNA is a thermosensor that modulates translation of the cold-shock protein CspA. *Mol. Cell*, **37**, 21–33.
41. Su,L.J., Brenowitz,M. and Pyle,A.M. (2003) An alternative route for the folding of large RNAs: apparent two-state folding by a group II intron ribozyme. *J. Mol. Biol.*, **334**, 639–652.
42. Qin,P.Z. and Pyle,A.M. (1997) Stopped-flow fluorescence spectroscopy of a group II intron ribozyme reveals that domain 1 is an independent folding unit with a requirement for specific Mg2+ ions in the tertiary structure. *Biochemistry*, **36**, 4718–4730.
43. Waldsich,C. and Pyle,A.M. (2007) A folding control element for tertiary collapse of a group II intron ribozyme. *Nat. Struct. Mol. Biol.*, **14**, 37–44.
44. Matsuura,M., Noah,J.W. and Lambowitz,A.M. (2001) Mechanism of maturase-promoted group II intron splicing. *EMBO J.*, **20**, 7259–7270.
45. Lindquist,J.A. and Mertens,P.R. (2018) Cold shock proteins: from cellular mechanisms to pathophysiology and disease. *Cell Commun. Signal.*, **16**, 63.
46. Toor,N., Hausner,G. and Zimmerly,S. (2001) Coevolution of group II intron RNA structures with their intron-encoded reverse transcriptases. *RNA*, **7**, 1142–1152.
47. Adamidi,C., Fedorova,O. and Pyle,A.M. (2003) A group II intron inserted into a bacterial heat-shock operon shows autocatalytic activity and unusual thermostability. *Biochemistry*, **42**, 3409–3418.
48. Qu,G., Dong,X., Piazza,C.L., Chalamcharla,V.R., Lutz,S., Curcio,M.J. and Belfort,M. (2014) RNA-RNA interactions and pre-mRNA mislocalization as drivers of group II intron loss from nuclear genomes. *Proc. Natl. Acad. Sci. U.S.A.*, **111**, 6612–6617.
49. Cech,T.R. (2009) Crawling out of the RNA world. *Cell*, **136**, 599–602.
50. Preussner,M., Goldammer,G., Neumann,A., Haltenhof,T., Rautenstrauch,P., Muller-McNicoll,M. and Heyd,F. (2017) Body temperature cycles control rhythmic alternative splicing in mammals. *Mol. Cell*, **67**, 433–446.
51. Gotic,I., Omidi,S., Fleury-Olela,F., Molina,N., Naef,F. and Schibler,U. (2016) Temperature regulates splicing efficiency of the cold-inducible RNA-binding protein gene Cirbp. *Genes Dev.*, **30**, 2005–2017.
52. Takayama,K. and Kjelleberg,S. (2000) The role of RNA stability during bacterial stress responses and starvation. *Environ. Microbiol.*, **2**, 355–365.
53. Chursov,A., Kopetzky,S.J., Bocharov,G., Frishman,D. and Shneider,A. (2013) RNAtips: Analysis of temperature-induced changes of RNA secondary structure. *Nucleic Acids Res.*, **41**, W486–491.
54. Nouaille,S., Mondeil,S., Finoux,A.L., Moulis,C., Girbal,L. and Cocaign-Bousquet,M. (2017) The stability of an mRNA is influenced by its concentration: a potential physical mechanism to regulate gene expression. *Nucleic Acids Res.*, **45**, 11711–11724.
55. Miousse,I.R., Chalbot,M.C., Lumen,A., Ferguson,A., Kavouras,I.G. and Koturbash,I. (2015) Response of transposable elements to environmental stressors. *Mutat Res Rev Mutat Res*, **765**, 19–39.
56. Singh,P.K. and Meijer,W.J. (2014) Diverse regulatory circuits for transfer of conjugative elements. *FEMS Microbiol. Lett.*, **358**, 119–128.
57. Beuls,E., Modrie,P., Deserranno,C. and Mahillon,J. (2012) High-salt stress conditions increase the pAW63 transfer frequency in *Bacillus thuringiensis*. *Appl. Environ. Microbiol.*, **78**, 7128–7131.
58. Cairns,J., Jalasvuori,M., Ojala,V., Brockhurst,M. and Hiltunen,T. (2016) Conjugation is necessary for a bacterial plasmid to survive under protozoan predation. *Biol. Lett.*, **12**, 20150953.